EDDY CURRENT INDUCTION BY A COIL NEAR A CONDUCTING EDGE IN 2D

S.K. Burke

Aeronautical Research Laboratories
Department of Defence
Melbourne, Australia.

INTRODUCTION

Difficulties often occur in eddy current inspection when a defect is situated close to an edge. This is due to the large signal arising from the edge ('edge-effect') which tends to obscure any signals coming from the defect[1,2]. To understand the edge-effect in eddy current NDI in more detail, the induction of eddy currents in a conducting 90° edge by a two-dimensional coil is considered in this paper. Firstly, the impedance of a two-dimensional coil in the vicinity of a conducting quarter-space is calculated numerically using a dual boundary-integral-equation (BIE) method and the results compared with experiment. The behaviour of the induced currents (vector potential) in the vicinity of the edge is then examined using the numerical (BIE) results and the results of an analytical approximation [3] valid in the limit of small skin-depth.

NUMERICAL CALCULATION OF COIL IMPEDANCE

The calculation of coil impedance was performed for the case shown in Fig. 1. A two-dimensional coil consisting to two identical rectangular windings is located near a uniform quarter-space ($x \geq 0$, $y \leq 0$) with conductivity σ and magnetic permeability μ_o. The coil windings carry equal and opposite alternating current $\pm Ie^{i\omega t}$, the centres of the windings are separated by a distance 2D and the windings have a turn density N/(4WT). The base of the coil is parallel to the top surface of the conductor, the coil 'liftoff' is H and the coil centreline is situated at a distance XC from the edge. In this two-dimensional idealization, the coil and quarter space are infinite in length normal to the X-Y plane; the coil windings may be visualized as a superposition of line-current sources.

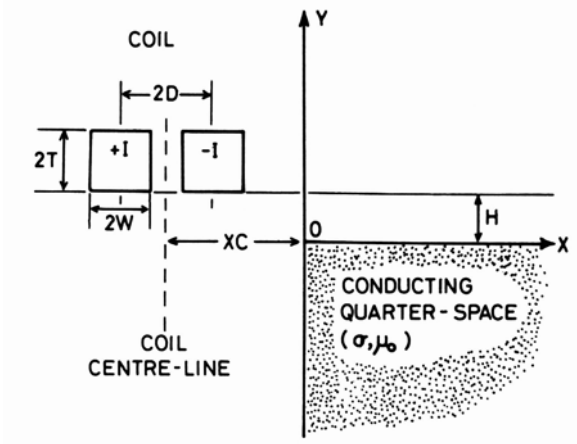

Fig. 1. Two-dimensional coil conducting quarter-space. Here XC is defined as positive when the coil is over the conductor.

The calculation of coil impedance closely follows the BIE method described by Kahn[4], who reduces the problem of obtaining the quasi-static electric and magnetic field to that of solving a pair of simultaneous integral equations for the z component of the magnetic vector potential (A) and its normal derivative ($\partial A/\partial n$) on the boundary of a conductor. These equations are,

$$\tfrac{1}{2} A(s) - \int_B ds' \frac{\partial G(s,s')}{\partial n'} A(s') + \int_B ds' G(s,s') \frac{\partial A}{\partial n'}(s') = A^\circ(s) \qquad (1)$$

$$\tfrac{1}{2} A(s) + \int_B ds' \frac{\partial g(s,s')}{\partial n'} A(s') - \int_B ds' g(s,s') \frac{\partial A}{\partial n'}(s') = 0 \qquad (2)$$

where

$$G(s,s') = -(2\pi)^{-1} \ln |s-s'|, \quad g(s,s') = (2\pi)^{-1} K_o (k|s-s'|), \quad k = (i\omega\mu_o\sigma)^{\frac{1}{2}}$$

and $A^\circ(s)$ is the (known) incident vector potential on the boundary. The integrations are over the conductor boundary (B) and the normal derivative is defined to be outward from the conductor. The coil impedance per unit length, Z, can be expressed in terms of A and $\partial A/\partial n$ obtained from the solution of equations 1-2 as follows,[5]

$$Z = \frac{i\omega}{\mu_o I^2} \int_B ds \left[A(s) \frac{\partial A^\circ(s)}{\partial n} - A^\circ(s) \frac{\partial A(s)}{\partial n}\right] + Z_o \qquad (3)$$

where Z_o is the coil impedance (per unit length) for the coil in isolation.

A system of coupled integral equations such as eq.1-2 can only realistically be solved by numerical methods and a variety of numerical techniques of greater or lesser sophistication may be used. All of these methods, however, rely on reducing the coupled integral equations to a set of simultaneous linear algebraic equations. The method which is adopted is similar to that employed by Kahn [4], using a point matching scheme but with triangular hat basis functions rather than triple-pulse hat basis functions.

To implement this scheme, a grid of variable size was used. Close to the edge and in the immediate vicinity of the coil a fine mesh was em-

ployed, whereas at large distances from the edge a coarse grid was used. A grid of intermediate width was used elsewhere and no grid point was placed on the edge itself. For satisfactory convergence it was necessary to extend the grid to large distances from the edge. The diagonal matrix elements and matrix elements involving $G(s,s')$ were calculated from exact analytical results. Accurate series and asymptotic expansions were used to calculate the off-diagonal matrix elements involving $g(s,s')$. Recalling that A and $\partial A/\partial n$ are phasors (complex) it proved convenient to code the system of simultaneous equations as COMPLEX variables and a Nag library routine [6] (f04adf) was used to solve this system numerically. The coil impedance was then calculated via eq.3, approximating the integral by using the trapeziodal rule. No significant change in the solution was found on increasing n above 200 points for a typical set of grid points.

EXPERIMENTAL VERIFICATION

The validity of these calculations was tested experimentally by measuring the impedance of a 'two-dimensional' coil in the vicinity of a 90° conducting edge. A rectangular coil of length 40.1cm was wound with N=158 turns of 'litz' wire. The coil dimensions (see Fig.1) were: 2D=1.02cm, 2W=0.84cm and 2T=0.95cm. As the coil had a large aspect ratio (40) it was essentially two-dimensional[3]. The inductance of the coil in isolation (L_o) was 3.50mH, in resonable agreement with the theoretical value of 3.87mH calculated for a two-dimensional coil of this size.

The experiments were performed on a large aluminium alloy block (1m x 1m x 11cm) with a resistivity of 5.4 μΩ cm. The coil impedance was measured, using an HP-4192A low-frequency impedance analyser, as the coil was translated along the top-surface of the block and across the edge with the base of the coil maintained at constant Y=H=1.3mm (refer Fig.1.) Data were collected at frequencies of 25kHz and 1kHz, corresponding to skin-depths ($\delta=\sqrt{2}/|k|$) of 0.74mm and 3.7mm respectively. The results are shown in Figures 2-3 and are in excellent agreement with the (parameter-free) numerical calculations.

THE EDGE EFFECT AND INDUCED FIELDS

The most significant feature of these results is that, while the coil reactance increases monotonically as the coil is translated across the edge, the resistance peaks before decreasing. This is the so-called 'edge-effect'.

This enhancement of the coil resistance can be traced to a concentration of the induced fields at the edge itself, analogous to the concentration of charge near a sharp edge in electrostatics. This is illustrated in Fig. 4 where the variation of the magnetic vector potential on the conductor surface, obtained from the numerical results for the 25kHz data set, is shown for selected values of coil center translation (XC). Two calculated curves are also shown here. The first represents the results of an approximate analytical calculation[3] for the vector potential on the conductor surface to first order in δ, $A \approx (1-i)\delta A'' + \ldots$ This approximation is in very good agreement with the numerical results for Re(A), the poorer agreement with Im(A) reflects the fact that the next term in the expansion for Im(A) is of order δ^2 whereas the next term for Re(A) is of order δ^3 for small δ. It should be noted that the vector potential in this small δ limit has a singularity of order -1/3 at the edge. The second set of curves in Fig. 4 represent the vector potential for the coil on an infinite half-space and are the result of an exact analytical calculation.[7]

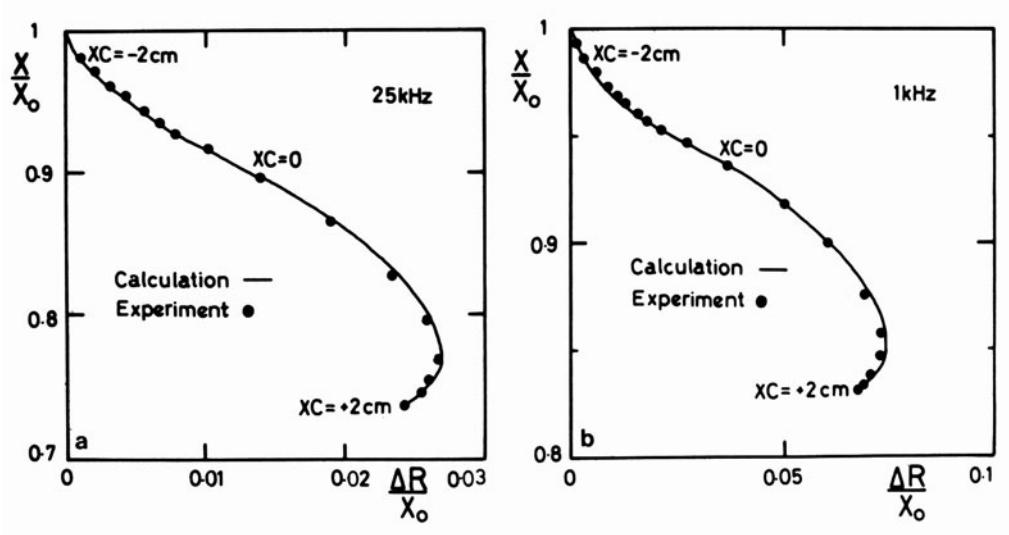

Fig. 2. Edge-effect loci in the normalized impedance plane for frequencies of (a) 25kHz and (b) 1 kHz. The solid circles are the experimental results and the curves are the results of the numerical calculation. The coil reatance (X) and change in coil resistance (Δ R) are normalized to the isolated coil reactance ($X_o=\omega L_o$) following the usual convention.

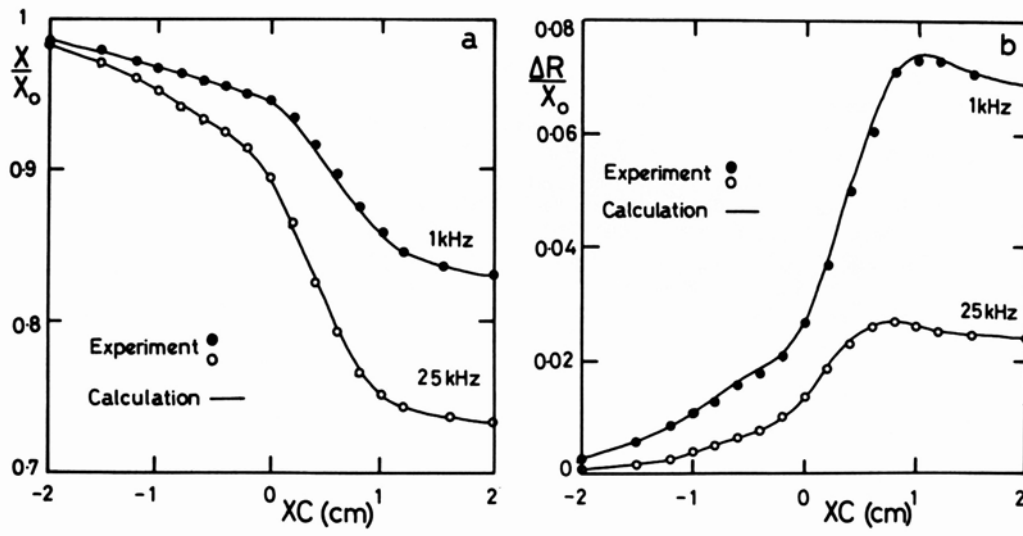

Fig. 3. Normalized coil reactance (a) and resistance (b) as a function of coil translation (XC) near a 90° edge for frequencies of 25kHz and 1kHz. The circles are the experimental data and the solid lines are the results of the numerical calculation.

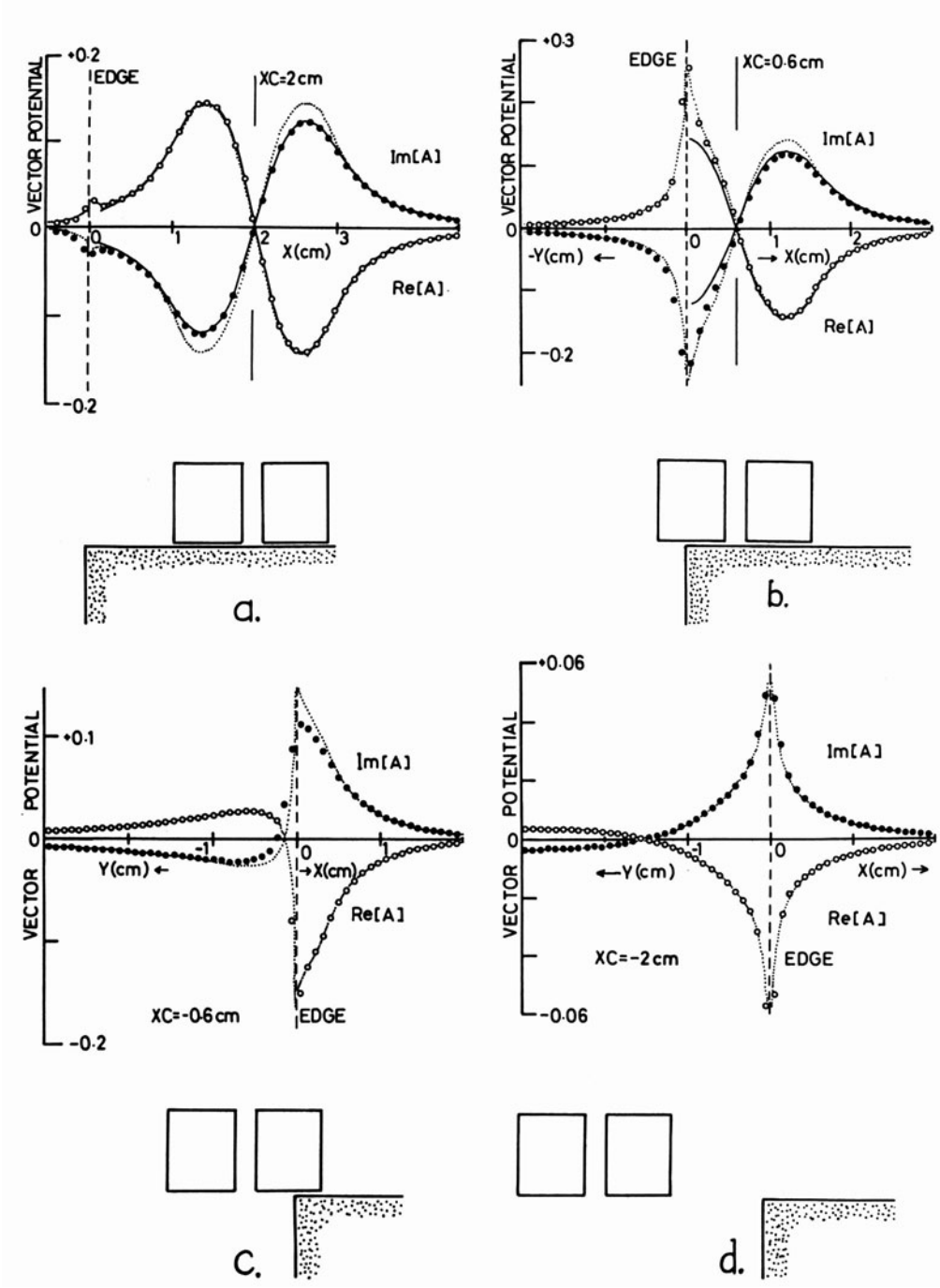

Fig. 4. Calculated vector potential on the surface of the aluminium alloy block. Real (o) and Imaginary (•) parts of A obtained numerically for the 25kHz data-set are plotted as a function of surface position for coil centre positions (XC) of (a) 2cm (b) 0.6cm (c) -0.6cm and (d) -2.0cm. Also shown are the results of the small skin-depth approximation for a 90° edge (dotted line) and the exact analytical calculation the coil on a half-space (solid line). Note the changes in scale.

The variation of vector potential on the conductor surface as the coil is translated across the edge may be described as follows. For XC=2cm, the coil is resting on the block at some distance from the edge and the vector potential on the top surface (X>0) is indistinguishable from that obtained from the exact calculations for a 2D coil in a half-space [7], except for a small increase close to the edge. This edge contribution increases significantly in size as the coil is moved closer to the edge of the block. This is illustrated in Fig. 4b where XC=0.6cm and the coil resistance is close to its maximum value. At this position the left-hand coil winding is centred on the edge, the incident vector potential at the edge is thus a maximum and a large edge response could be expected. The vector potential on the top surface approaches the half-space values for X>XC (i.e. beyond the coil centre) but is significantly larger near the edge. As the coil is translated across the edge and off the block, the vector potential decreases rapidly. When the right-hand coil winding is centred on the edge (XC=-0.6cm) an enhanced edge contribution is observed, corresponding to the weak 'shoulder' seen in the coil resistance-position curves in Fig. 3b. The tendency for the vector potential (or induced current) to be concentrated near the edge is well illustrated in Fig.4d, where the coil is distant from the edge (XC=-2cm).

To account for the variation of coil impedance with position it is convenient to turn to an alternative expression [8],

$$Z = \frac{i\omega}{I} \frac{N}{4WT} \left[\iint_{(+)} A \, dxdy - \iint_{(-)} A \, dxdy \right] \qquad (6)$$

which relates the impedance to the integral of the vector potential over the coil windings (denoted (+) and (-)), rather than using the surface integral formulation of equation 3. This expression, taken with the fact that Im(A) decays smoothly out from the conductor surface, implies that the peak in the coil resistance is a direct consequence of the enhancement of Im(A) at the conductor edge. The coil reactance, however, shows no such peak and increases rapidly as the coil is translated across the edge. This difference in behaviour is most easily understood by considering the small δ expansion for A outside (and on) the conductor [3],

$$A = A' + (1-i)\delta A'' + \ldots . \qquad (7)$$

A', the vector potential in the perfect conductor limit ($\delta = 0$), is purely real and is zero on the conductor surface. The second term, which consists of equal and opposite real and imaginary parts, was shown for selected values of XC in Fig 4. Re(A) at the coil windings, which determines the coil reactance is dominated by A' and any edge contributions from A'' show up as a weak 'shoulder' in the reactance-position curve.

These results for a 2D coil are relevant to those 3D geometries in which a significant proportion of induced current flows parallel to a conducting edge, as for example is the case for a pancake coil resting flat on the conductor surface and with the coil centre not too close to the edge.

CONCLUSION

The impedance of a two-dimensional coil in the vicinity of a homogenous conducting quarter-space was calculated using a dual boundary-integral-equation method. The results were in excellent agreement with a series of experiments performed using a rectangular coil of large aspect ratio which approximated to a 2D coil. The behaviour of the vector-potential on the conductor surface was considered in detail and the maximum in coil resistance was traced to the concentration of A near the edge.

REFERENCES

1. B. C. Bishop and N. T. Goldsmith, Non-Destructive Testing Australia 21 2 6-8 (1984).
2. D. J. A. Williams, J. P. Tilson and J. Blitz, Effects of the Edges of Samples on Eddy-Current Flaw Evaluation, in Proceedings of Fourteenth Symposium on Nondestructive Evaluation, (San Antonio, Texas, 1983).
3. S. K. Burke, J. Phys. D: Appl. Phys. 18 1745-60 (1985).
4. A. H. Kahn, J. Res. National Bureau of Standards 89 47-54 (1984).
5. B. A. Auld, Theoretical Characterization and Comparison of Resonant Probe Microwave Eddy-Current Testing with Conventional Low Frequency Eddy-Current Methods, in Eddy-Current Characterization of Materials and Structures, ASTM STP 722, eds., G. Birnbaum and G. Free, (American Society for Testing and Materials, Philadelphia, 1981), 332-347.
6. Nag Fortran Library MK 11, Numerical Algorithms Group, 256 Banbury Rd., Oxford, OX2 7DE UK.
7. Induction by a current filament above a half-space is treated by many authors (e.g. J. A. Tegopoulos and E. E. Kriezis, "Eddy Currents in Linear Conducting Media. Studies in Electrical and Electronic Engineering 16" (Elsevier, Amsterdam, 1985), p. 89ff). Results for a coil of finite cross-section are obtained by superposition.
8. C. V. Dodd and W. E. Deeds, J. Appl. Phys. 39 2829-38 (1968).